Modeling on-grate MSW incineration with experimental validation in a batch incinerator

ASTHANA, Abhishek, MÉNARD, Y, SESSIECQ, P and PATISSON, F

Modeling On-Grate MSW Incineration with Experimental Validation in a Batch Incinerator

Abhishek Asthana, Yannick Ménard, Philippe Sessiecq, and Fabrice Patisson*

Institut Jean Lamour, CNRS, Nancy-Université, Nancy, France

This Article presents a 2-D steady-state model developed for simulating on-grate municipal solid waste incineration, termed GARBED-ss. Gas−solid reactions, gas flow through the porous waste particle bed, conductive, convective, and radiative heat transfer, drying and pyrolysis of the feed, the emission of volatile species, combustion of the pyrolysis gases, the formation and oxidation of char and its gasification by water vapor and carbon dioxide, and the consequent reduction of the bed volume are described in the bed model. The kinetics of the pyrolysis of cellulosic and noncellulosic materials were experimentally derived from experimental measurements. The simulation results provide a deep insight into the various phenomena involved in incineration, for example, the complete consumption of oxygen in a large zone of the bed and a consequent char-gasification zone. The model was successfully validated against experimental measurements in a laboratory batch reactor, using an adapted sister version in a transient regime.

Introduction

The bed of refuse particles that burns on the grate of the incinerator is the real heart of the municipal solid waste (MSW) incineration process. It is the place where waste-to-energy conversion occurs and the refuse is reduced into ash, but also the place where most of the pollutants (NO_x, heavy metals, etc.) are released. Detailed knowledge of what exactly happens when the bed is incinerated is therefore highly desirable before strategies for controlling and optimizing the process can be proposed. This knowledge cannot be readily obtained from direct experimental studies on industrial-scale incinerators; in contrast, mathematical modeling and numerical simulation appear to be an attractive approach for quantitative insight into the mechanisms and variables of waste-bed incineration.

This stated, and probably because modeling such an ill-defined fuel and complex apparatus seems to be a challenging task, reports of mathematical models of MSW bed combustion are few.[1−4] Since the pioneering work of Essenhigh,[1] however, these models have become more sophisticated in their description of the physical and chemical phenomena, that is, heat transfer, gas flow, drying, pyrolysis, combustion of gases and of char, bed shrinkage, and sometimes bed mixing. Most are one-dimensional and transient, which is a proper description of the batch incineration of a fixed bed, but insufficient if modeling of the gas and solid flows, or just of bed mixing, is intended. The most advanced work to date is that of Sheffield University, UK, which actually gave birth to the software named FLIC.[4,5] This model describes most of the phenomena involved and uses kinetic data from the literature; for example, pyrolysis kinetics are taken from literature data obtained in the case of coal.

When developing the present model, we took advantage of the most relevant descriptions of earlier studies. Whenever possible, we also tried to improve the modeling, for example, when selecting pyrolysis kinetics derived from dedicated experiments, adding the reactions of char gasification, refining the description of char combustion, writing a 2-D model, and offering the possibility of simulating the stirring of the bed. The aim was to develop a comprehensive, state-of-the-art model, based on experiments and validated against experiments, whose detailed features are given in the present Article.

Beyond enlightening us on the behavior of the burning waste bed, a bed model should be designed to be usefully coupled to a model of the remaining sections of the incinerator, the postcombustion chamber and the boiler, to enable a full simulation of industrial units. This approach was successfully employed for grate[6] or rotary kiln[7] plants. We used it for predicting the speciation of heavy metals throughout the furnace.[8]

Mathematical Model of MSW Bed Combustion

The present bed model, developed into software registered as GARBED-ss, is two-dimensional and steady state. It describes most of the actual physical, chemical, and thermal phenomena (Figure 1) taking place in a burning MSW bed, for example, solid and gas flow, drying and pyrolysis of the feed, combustion of the gases released from pyrolysis, formation of a carbonaceous residue (char) and its subsequent degradation by gasification and combustion, heat transfer, and particle and bed shrinkage.

The following assumptions were made to simplify the description of these phenomena. The feed advances on the

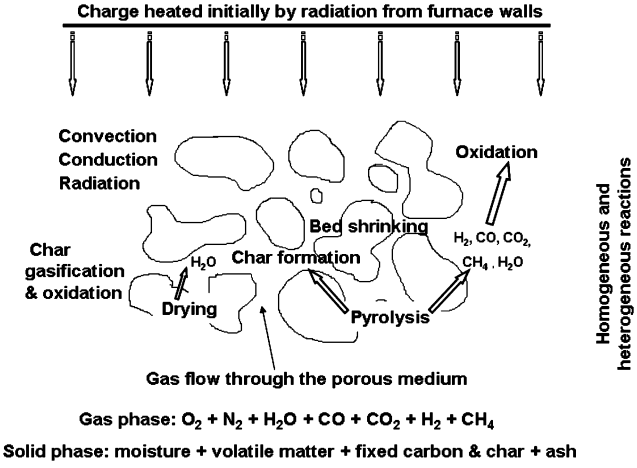

Figure 1. The physical, chemical, and thermal phenomena taking place in the bed under combustion.

* To whom correspondence should be addressed. Tel.: (33) 383584267. Fax: (33) 383584056. E-mail: fabrice.patisson@mines.inpl-nancy.fr.

10.1021/ie100175e

Table 1. Local Balance Equations Solved in GARBED-ss

heat, solid

$$v_s\rho_{app,s}c_{ps}\frac{\partial T_s}{\partial x} - \frac{\partial}{\partial x}\left(\lambda_{eff}\frac{\partial T_s}{\partial x}\right) - \frac{\partial}{\partial z}\left(\lambda_{eff}\frac{\partial T_s}{\partial z}\right) = a_g h(T_g - T_s) - \sum_{i\in\{\text{all heterogeneous reactions}\}} r_i\Delta_r h_i + S_{rad} \quad (1)$$

v_s = velocity of the solid (subscript s) feed, m s^{-1}; $\rho_{app,s}$ = apparent density, kg m^{-3}; c_{ps} = specific heat, J kg^{-1} K^{-1}; T_s = temperature, K; x = distance along the grate, m; λ_{eff} = effective thermal conductivity, W m^{-1} K^{-1}; z = height in the bed, m; a_g = specific surface area of the bed, m^{-1}; h = gas−solid heat-transfer coefficient, W m^{-2} K^{-1}; r_i = rate of reaction i, kg s^{-1} m^{-3}; $\Delta_r h_i$ = heat of reaction i, J kg^{-1}; S_{rad} = source term due to radiation, W m^{-3}

heat, gas

$$v_{g,x}\rho_g c_{pg}\frac{\partial T_g}{\partial x} + v_{g,z}\rho_g c_{pg}\frac{\partial T_g}{\partial z} = a_g h(T_s - T_g) - \sum_{i\in\{CH_4,CO,H_2\}} \varepsilon_b r_i^*\Delta_r h_i^* + \sum_{i\in\{\text{all gas species}\}} \varepsilon_b r^*_{prod,i}\int_{T_g}^{T_s} c^*_{p_i}\,dT \quad (2)$$

$v_{g,x}$ = horizontal superficial velocity of the gas (subscript g), m s^{-1}; ρ_g = density, kg m^{-3}; c_{pg} = specific heat, J kg^{-1} K^{-1}; T_g = temperature, K; $v_{g,z}$ = vertical superficial velocity, m s^{-1}; ε_b = porosity of the bed; r_i^* = molar rate of combustion of species i, mol s^{-1} m^{-3}; $\Delta_r h_i^*$ = molar heat of reaction, J mol^{-1}; $r^*_{prod,i}$ = net molar rate of production of species i by all heterogeneous reactions, mol s^{-1} m^{-3}; c_{pi}^* = molar specific heat, J mol^{-1} K^{-1}

mass, solids

$$\frac{\partial}{\partial x}(\rho_{app,s}v_s w_i) = S_{w_i}, \quad i \in \{\text{moisture, volatile matter, char or ash}\} \quad (3)$$

w_i = mass fraction of component i in the solid; S_{w_i} = net rate of production of i by heterogeneous reactions, kg s^{-1} m^{-3}

mass, gases

$$\frac{\partial}{\partial x}(\rho_g v_{g,x} y_i) + \frac{\partial}{\partial z}(\rho_g v_{g,z} y_i) = S_{y_i}, \quad i \in \{\text{all gaseous species}\} \quad (4)$$

y_i = mass fraction of species i in the gas; S_{y_i} = net rate of production of i by all reactions involving it, kg s^{-1} m^{-3}

momentum, gas

$$-\frac{\partial}{\partial x}\left(\frac{KM_g}{2RT_g\mu_g}\frac{\partial p^2}{\partial x}\right) - \frac{\partial}{\partial z}\left(\frac{KM_g}{2RT_g\mu_g}\frac{\partial p^2}{\partial z}\right) = \sum_{i\in\{\text{all gas species}\}} S_{y_i} \quad (5)$$

K = permeability of the bed, m^2; M_g = molar weight of the gas mixture, kg mol^{-1}; p = gas pressure, Pa; R = ideal gas constant, J mol^{-1} K^{-1}; μ_g = gas viscosity, kg m^{-1} s^{-1}

moving grate parallel to the grate and at constant velocity, except when stirring is considered. Primary air (the air for combustion) is injected into the incinerator under the moving grate. The solid bed is considered to be a porous medium made up of spherical particles, which allows gas to flow through it. The MSW feed consists of moisture, fixed carbon, volatile matter, and inert matter or ash. The gas phase consists of oxygen, nitrogen, water vapor, carbon monoxide, carbon dioxide, methane, and hydrogen. Gas and solid temperatures are considered separately. Heat transfer in the bed takes place by convection, conduction, and radiation.

The solid feed, as it advances over the moving grate, is first dried and then devolatilized. The latter process, often termed pyrolysis although oxygen is present in this case, releases volatile gases (H_2O, CO_2, CO, H_2, and CH_4) and leaves behind a carbonaceous residue (char). Pyrolysis gases burn with the oxygen injected as the primary air. Char also burns with oxygen when the latter is available; otherwise, it can be gasified by H_2O and CO_2. Gasification has been ignored in previous models, whereas our results show its significant contribution. The final solid particles after complete combustion, that is, the bottom ash, or slag, correspond to the inert part of the initial feed. The significant decrease in bed volume is modeled through a progressive shrinkage of the waste particles. Optionally, stirring of the feed, which is superimposed on its axial progression, is accounted for.

Writing and solving the local balance equations expressing the conservation of momentum, energy, and mass form the basis of the model. The relevant equations are listed in Table 1, and the source terms corresponding to the various heterogeneous and homogeneous reactions considered are given in Table 2. The next paragraphs explain in more detail how the various physical, chemical, and thermal phenomena are modeled and how their rates are determined.

Heat Transfer. The solid waste particles are considered uniform in temperature, as justified by a particle Biot number lower than 0.1 under typical incineration conditions.[9] Particles in the bed exchange heat with their neighbors by conduction and radiation. Radiation is the primary mode of heat transfer in the layers under combustion. Radiation coming from the walls of the incinerator furnace and the flame initiates the combustion of the upper layers of the waste bed. Inside the bed, associated with conduction, radiation allows the flame front to progress downward, opposite to the gas flow. An expression for the source term for radiation S_{rad} and correlations for calculating the effective conductivity of the bed (calculated values ranging from 0.5 to 60 W m^{-1} K^{-1}) are given by Asthana[14] and are also available in the Supporting Information. In the gas phase, heat transfer by conduction is negligible as compared to convection, as justified by a particle Péclet number greater than 50. The gas−solid heat-exchange coefficient h (calculated values ranging from 5 to 60 W m^{-2} K^{-1}) is obtained from the relation of Wakao and Kaguei.[15] The heat of the heterogeneous reactions is attributed to the solid phase as these reactions take place either inside the porous particles or at their surface.

Table 2. Main Transformations Considered in the Model and Their Rates

	mechanism		rate		ref
drying	$H_2O_{liq,in\ solid} \rightarrow H_2O_g$	(6a)	$r_{drying} = \frac{k_m a_g M_{H_2O}}{RT_g}(p_{H_2O,surf} - p_{H_2O})$	(6b)	9
			k_m = mass-transfer coefficient, m s^{-1}; p_{H_2O} = partial pressure of water vapor (subscript surf: at the particle surface), Pa		
pyrolysis	$1kg_{volatile\ matter} \rightarrow \alpha_{CH_4}kg_{CH_4} + \alpha_{H_2}kg_{H_2} + \alpha_{CO}kg_{CO} + \alpha_{CO_2}kg_{CO_2} + \alpha_{H_2O}kg_{H_2O}$	(7a)	$r_{pyro} = 225.7e^{-16375/R(\frac{1}{T_s}-\frac{1}{1000})}\rho_{app}w_{cell} + 0.045e^{-3230/R(\frac{1}{T_s}-\frac{1}{1000})}\rho_{app}w_{ncell}$	(7b)	10
	α_i = mass of i produced by the pyrolysis of 1 kg of volatile matter; see Table S1 of the Supporting Information for the values		w_{cell}, w_{ncell} = mass fractions of cellulosic and noncellulosic matter		
gas combustion	$CH_4 + \frac{3}{2}O_2 \rightarrow CO + 2H_2O$	(8a)	$r^*_{CH_4} = 1.5 \times 10^8 e^{-200800/RT_g}c_{CH_4}^{0.7}c_{O_2}^{0.8}$	(8b)	11
			c_i = molar concentration of i, mol m^{-3}		
	$CO + \frac{1}{2}O_2 \rightarrow CO_2$	(9a)	$r^*_{CO} = 1.3 \times 10^8 e^{-125500/RT_g}c_{CO}c_{O_2}^{0.5}c_{H_2O}^{0.5}$	(9b)	12
	$H_2 + \frac{1}{2}O_2 \rightarrow H_2O$	(10a)	$r^*_{H_2} = 1.1 \times 10^{13} e^{-75000/RT_g}c_{H_2}c_{O_2}$	(10b)	13
char combustion	$C + \gamma O_2 \rightarrow (2\gamma - 1)CO_2 + 2(1 - \gamma)CO$	(11a)	$r_{comb,C} = a_g\left(\frac{e^{b_{O_2}}}{\Omega_{act}r_{C,chem}} + \frac{e^{b_{O_2}} - 1}{b_{O_2}r_{C,diff}}\right)^{-1}$	(11b)	9
	see the Supporting Infromation for the way of determining γ		b_{O2} = Péclet number for Stefan flow; Ω_{act} = fractional reduction of reaction surface area; subscripts: chem = chemical reaction, diff = diffusion		
char gasification	$C + H_2O \rightarrow CO + H_2$	(12a)	$r_{gas,i} = a_g\left(\frac{e^{b_i}}{\Omega_{act}r_{gas,i,chem}} + \frac{e^{b_i} - 1}{\Omega_{act}r_{gas,i,diff}}\right)^{-1}$	(12c)	9
	$C + CO_2 \rightarrow 2CO$	(12b)	$i = H_2O$ or CO_2		

Drying. Like Shin and Choi,[3] we assume that drying takes place in the "constant-rate" regime, where the rate is determined by the external mass transfer, as expressed in Table 2, eq 6b. Formulas for calculating the mass-transfer coefficient[15] and the saturation pressure are given in the Supporting Information.

Pyrolysis. During pyrolysis, the organic matter is decomposed and, as temperature increases, partitioned into volatile matter, that is, gases and tar, and a carbonaceous residue, char. At high heating rates or high temperatures, tar is in turn cracked into lighter gaseous species. If oxygen is present, most of the species evolved are directly oxidized. Globally, for our purpose, the decomposition of volatile matter can be considered to produce a mixture of gases and char. Gas composition and the respective amounts of gases and char depend on kinetic factors related to both the solid fuel and the local decomposition conditions, particularly the heating rate. Considerable research work addressed this issue. In MSW-incineration studies, the simplest representations used a constant decomposition temperature[2] or a single Arrhenius-type equation for all of the constituents with coefficients taken from experimental studies on wood.[3] The most advanced of these[4] uses the model of distributed activation energies, which introduces a stochastic variable into the rate law in the form of a distribution of activation energies[16] but with numerical coefficients corresponding to data on coal. We decided to use the model of Garcia et al.,[10] which was specifically developed for interpreting MSW-pyrolysis experiments and which accurately reflected our experimental results on the pyrolysis kinetics of MSW samples (as shown in the Supporting Information). This model distinguishes between cellulosic (wood, paper, cardboard, etc.) and noncellulosic fractions in MSW and attributes to each fraction its own kinetics (Table 2, eq 7b). Furthermore, predicting the composition of the gas mixture released from reaction mechanisms alone still eludes current models, particularly in the case of MSW pyrolysis. The composition has to be fixed a priori; we calculated the set of α_i (see Supporting Information) to satisfy the elemental composition and calorific value of MSW.

Oxidation of Pyrolysis Gases. The combustible gaseous species released from pyrolysis directly burn with the oxygen of the primary air. Global rate equations for these homogeneous combustion reactions are available from the literature (Table 2, eqs 8b−10b).

Combustion of Char. Like coal pyrolysis, coal, coke, and char combustion have been extensively studied, even though no specific study concerned the carbonaceous residue from MSW pyrolysis. This heterogeneous combustion produces CO and CO_2 in proportions that mostly depend on temperature. Arthur's law[17] is often used for determining the CO/CO_2 ratio as a function of temperature; we used a slightly more detailed relationship[18] to calculate it (see Supporting Information). In the conditions of MSW incineration, char combustion occurs in a mixed regime, limited by both reaction kinetics and external diffusion.[9] Following Rosendahl,[19] we introduced two refinements in the calculation of the reaction rate. The first was to consider that, as combustion progresses, the increase in ash content decreases the surface area available for reaction, which is reflected by the coefficient Ω_{act} in the rate expression presented Table 2, eq 11b. The second was to account for Stefan flow, that is, the perturbation to external mass transfer caused by the strong outward flow of the evolved gases. This introduces the factor b_{O_2}, a kind of Péclet number, in the same rate expression.

Gasification of Char. Gasification of carbon (char or coke) by steam is a well-known process for producing syngas. Both steam and carbon dioxide can gasify carbon according to the reactions written Table 2, eqs 12a,b, the steam reaction being typically thrice as fast.[20] Thermodynamic calculations indicate that these reactions

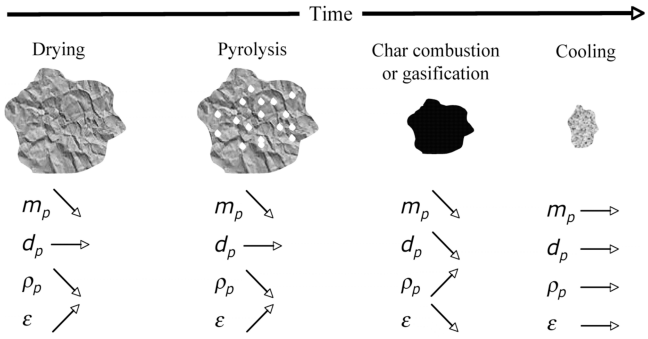

Figure 2. Evolution of a waste particle with time.

occur at high temperature with high H_2O and CO_2 concentrations. As will be shown, these conditions are those prevailing in a large section of the MSW bed in incineration. Therefore, despite these reactions having been, surprisingly, ignored in earlier models, they were taken into account in the present one. The kinetics were modeled with the same type of rate expressions as for char oxidation, because all three reactions proceed by heterogeneous consumption of the same solid.

Gas Flow through the Bed. The equation for momentum transfer through a packed particle bed such as MSW particles on the incinerator grate reduces to Darcy's law. When combined with the continuity equation, that is, the overall mass balance of the gas phase, the gas velocity can be eliminated to yield an equation in p^2 (Table 1, eq 5). The latter equation is solved to calculate the pressure field, and, from it, the gas velocities $v_{g,x}$ and $v_{g,z}$ are derived using Darcy's law.

Evolution of the Particles. The reduction in volume (typically 90%) and in mass (75%) of the MSW when incinerated is considerable and must obviously be appropriately described in a mathematical model. Goh et al. calculated the change in bed volume by considering the detailed evolution of six different components of MSW, one being the internal porosity of the waste particles;[2] we followed a similar approach. During drying and pyrolysis, it is assumed that the matter released is replaced by a new internal porosity, with the volume of the waste particle remaining constant (Goh et al. assumed the volume replacement of volatile matter was only partial). The reduction in particle and bed volume is then associated with the consumption of char, either by combustion or by gasification (Figure 2). The equations for calculating the volume, mass, density, and diameter of the particles are given in the Supporting Information. Additionally, the height of the grid cells used for the numerical solution also changes proportionally to the particle volume.

Stirring of the Bed. Most industrial-scale incinerators adopt the practice of mixing the fuel bed to decrease the time required for complete burn out and to eliminate any unburned chunks in the colder layers. An option for simulating feed stirring was introduced in GARBED-ss. As in the work of Ryu et al.,[21] stirring is modeled through a process of exchanging adjacent layers.[14] The resulting movement of the solid appears sinusoidal. Nakamura and Themelis studied the distribution of tracer particles in a waste bed stirred by alternating bars and reported a movement close to sinusoidal.[22,23]

Boundary Conditions. The partial derivative equations expressing the local balances require boundary conditions to be set for their solution. Solid and gas flow rates, temperatures, and compositions are known at their respective inlets, that is, under the feeder and under the grate. The grate temperature, the exact value of which has little influence on the calculation, is taken as the average between the temperatures of the inlet gas and of the first layer of solids. Pressure is known at the gas outlet, above the bed surface. Moreover, at the gas outlet, the diffusive fluxes are assumed negligible as compared to the convective ones, and the radiation flux received from the furnace walls above is taken as that of a gray body at 1000 C. The latter condition can be easily changed, and, whenever GARBED-ss code is coupled with furnace calculations, this radiative heat flux indeed becomes a result of the furnace simulation.

Numerical Solution. The partial derivative equations are rendered discrete and solved using the classical finite volume method.[24] The so-called upwind scheme and a Gauss−Seidel iterative method are employed. Two features of our work are more original: first, the solution of the pressure/velocity coupling through the p^2-equation presented above and, second, the adaptive grid, in which the height of cells shrinks with the advance of the combustion. The number of meshes (typically 150×75) was chosen as a compromise between accuracy and computing time. Convergence is reached after a few millions of iterations, when all relative residues become lower than a set criterion (typically 10^{-6}).

Results and Discussion

The calculations were applied to simulating the MSW bed of the incinerator in Strasbourg, France, during a typical operation. This incinerator uses three successive grates (1.15, 5.50, and 5.50 m long, respectively), which were combined into one in the results diagrams for the purpose of representation. The waste feed was 11 tons h^{-1}, the bed height 0.8 m, and the primary air flow rate 30 000 m^3_{STP} h^{-1}, injected at 25 C. The

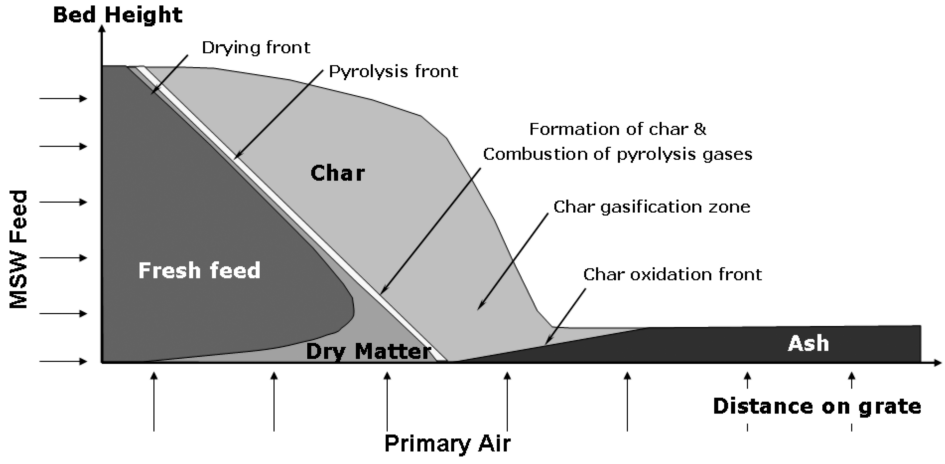

Figure 3. Synthesis of the distinct zones in the burning MSW bed, as predicted by the model.

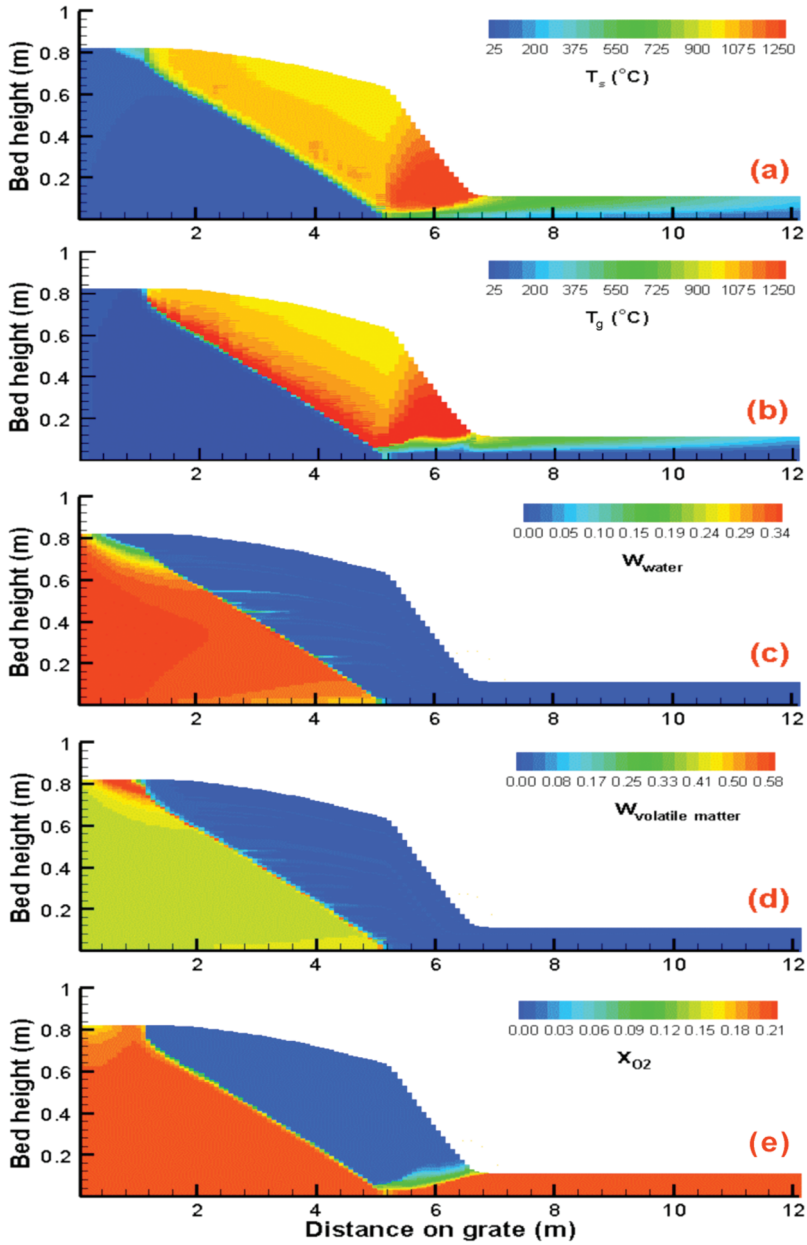

Figure 4. Main results from the model: (a) temperature of solid, (b) temperature of gas, (c) mass fraction of moisture in the solid, (d) mass fraction of volatile matter in the solid, and (e) mole fraction of oxygen in the gas phase.

complete operating conditions and feed characteristics are given in the Supporting Information.

The results calculated from the model include the solid and gas temperatures and compositions, gas pressure and velocity, and reaction rates, together with other secondary variables and parameters. It would have been impossible to measure any of these parameters experimentally at each point in real industrial or pilot incinerators. By calculating these variables from the model simulations, 2-D maps of isovalues (lines or contours) can be traced throughout the bed. An analysis of the entire set of results provides an insight into how and where the various transformations are taking place. A synthesis of the different zones found in the bed, as revealed by the model, is illustrated in Figure 3. In this diagram, as well as in all of the following ones, the axis representing the bed height has been magnified (5 times) for better legibility.

Five distinct zones separated by four fronts can be identified in the bed. Initially, the MSW feed containing moisture is dried. Pyrolysis immediately follows drying; the speed of this transformation limits it to a narrow zone, that is, the pyrolysis front. Above the pyrolysis front is the "active combustion zone" where the combustion of the gases released from pyrolysis takes place. In the zone above active combustion, oxygen is completely depleted (see Figure 4e), and the char left behind by pyrolysis can only be gasified by CO_2 or H_2O. The oxidation of char only begins downstream, at the last combustion front where oxygen again becomes available. The profile of the bed surface reflects the consumption of char either by gasification or by combustion. Such zones have already been identified in previous studies,[2,3] but not always distinguished in this way. In particular, the char-gasification zone is of a different shape and greater extent according to our calculations (see Figure 5c).

Figure 4 shows the main results including the contours of solid and gas temperatures, mass fractions of moisture and volatile matter in the solid, and mole fraction of oxygen in the gas phase for the standard operating conditions of the Strasbourg incinerator. Please note that the contour legends used in these figures may be misleading on proofs printed in black and white.

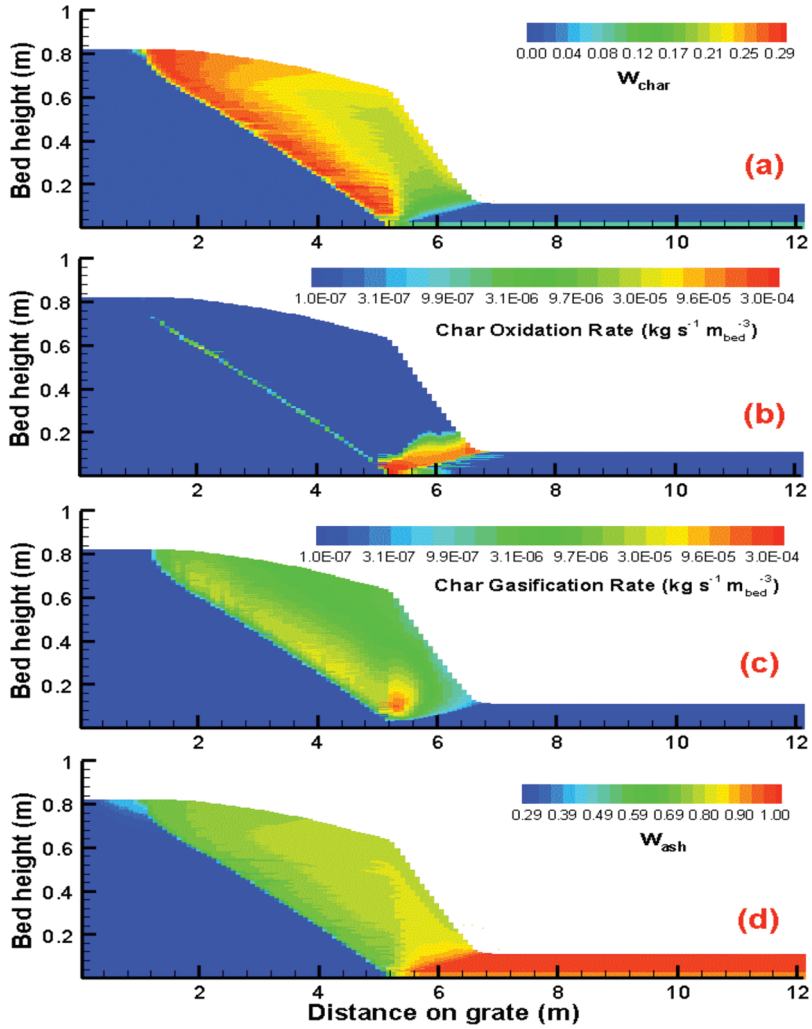

Figure 5. Char evolution: (a) mass fraction of char, (b) char oxidation rate, (c) char gasification rate, and (d) mass fraction of ash.

It can be seen that upstream of the drying front, the temperature of the solid does not increase significantly as the heat is consumed primarily for the vaporization of moisture present in the feed. Downstream of the drying and pyrolysis fronts, the temperatures suddenly rise because of the oxidation of gases released from pyrolysis, which is highly exothermic (Figure 4b). This oxidation of gases consumes all of the oxygen in the gas phase as can be seen in the form of a large reducing zone in Figure 4e. Only when this gas-combustion front reaches the grate (at about 5 m) does oxygen again become available for the oxidation of char. This char-oxidation zone is the hottest part of the waste bed, with a solid temperature of nearly 1200 C. The shapes of the temperature and water-content maps agree well with previous publications; however, it is not easy to further compare the full set of results with those of earlier studies, where generally only scarce isoline data were presented.

Figure 5 describes more precisely the processes of formation and destruction of char. Figure 5b and c is plotted with logarithmic scales. Char first appears in the bed at the pyrolysis front (Figure 5a). Next, as char is oxidized (Figure 5b) or gasified (Figure 5c), the bed height decreases and the mass fraction of ash in the bed increases (Figure 5d). A sharp fall in bed height can be noted between $x = 5$ and 6.4 m as the oxidation of char begins in this zone. In the oxygen-depleted zone downstream of the gas-combustion zone, char oxidation is not possible; the only consumption of char in this zone is by gasification. This makes the bed surface profile somewhat steeper than those found by others[4,21] but in agreement with observations made through the end window of the Strasbourg incinerator. Figure 5a and d also shows some unburned char in the bottom layers of ash near the grate. This is because of the relatively lower temperatures in this zone (cf., Figure 4a), which do not allow full oxidation of the char.

Figure 6 illustrates the 2-D nature of the gas-pressure and velocity fields. In industrial incineration practice, the total flow rate of the primary air is distributed among the different grate sections to optimize its use for combustion. In the case simulated, the three sections received 1%, 89%, and 10% of the total flow rate, respectively. The distribution of the primary air and the presence of large thermal gradients at the level of the combustion fronts cause horizontal pressure gradients in addition to the vertical ones. This entails a change in the direction of the gas flow, as shown by the velocity vectors that curve round under the fronts of combustion of the pyrolysis gases and of the char, which, because hot zones, are regions of lesser permeability. The interest of a truly 2-D model for correctly describing gas flow is thus clearly obvious.

These three results exemplify how the model helps us to understand in detail the processes involved in the combustion of a waste bed on a traveling grate, at a local scale where measurements would not be possible. Other simulation results, like the influence of several operating parameters (e.g., feed composition; total flow rate, distribution, and temperature of the primary air),[14] are not reported here for brevity's sake. Additionally, the calculated values of temperatures and com-

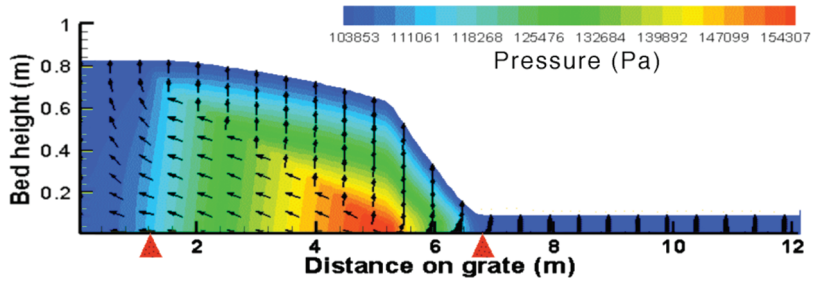

Figure 6. Gas flow: pressure and gas-velocity vectors. All vectors are plotted with the same magnitude for better legibility. The red triangles show the limits between the three sections of the grate.

positions form a valuable basis for further calculations regarding pollutant formation from MSW incineration.[8,25,26]

Experimental Validation of a Sister Transient Model

In the Strasbourg incinerator, the combustion is indeed completed at the end of the second grate, in good agreement with the model prediction. Other than this, a direct validation of the calculations by comparisons with measurements in on-grate industrial incinerators has not been possible as readings can be taken only at a few points, such as at the exits for the gases and the slag.

However, a sister version of the same bed model, in a transient regime (named GARBED-tr), aimed at simulating a batch incinerator was also written.[9] The equations were rewritten in cylindrical coordinates with additional accumulation terms to account for the transient regime. Apart from that, both mathematical models are otherwise identical. We therefore considered that validating the transient model against experiments would indirectly validate the steady-state model (the authors of other 1-D, transient, fixed-bed models have made the same assumption, but in the opposite way, when using this type of model for simulating incineration on a moving grate). Of course, further comparison of the steady-state model results with data measured on a full-scale plant would be welcome for reinforcing the validation.

Calculated results from the transient model were compared with experimental results from a fixed-bed batch pilot incinerator (KLEAA, at Forschungszentrum Karlsruhe, Germany). The pilot pot was cylindrical, with diameter and height each equal to 0.25 m. Thirteen thermocouples were placed within the pot, inside the solid bed at different heights at intervals of 1.5 cm. The primary air was injected under the pot through a grate at the bottom, and a gas analyzer was connected downstream of the gas vent at the top. The waste used in the experimental measurements was wood chips, whose composition is given in the Supporting Information, Table S2. A fairly good agreement was found between the model predictions and the experimental observations (Figures 7 and 8).

The consecutive abrupt rise in the temperatures of the thermocouples (TC_1 to TC_{13}, Figure 7) was a result of the propagation of the flame front. The rate of this propagation was well reproduced by the model. The slight differences between calculated and measured temperature values could be attributed to the sheaths of the thermocouples, which partly shielded them from radiation and increased their thermal inertia. A sudden increase in the temperatures recorded by the thermocouples between 1600 and 2000 s, as seen in both the experiments and the model predictions, was due to the oxidation of char, which is a highly exothermic reaction. The CO and CO_2 concentrations were well predicted by the model (Figure 8), and the pattern of oxygen evolution was reasonably well predicted. One significant

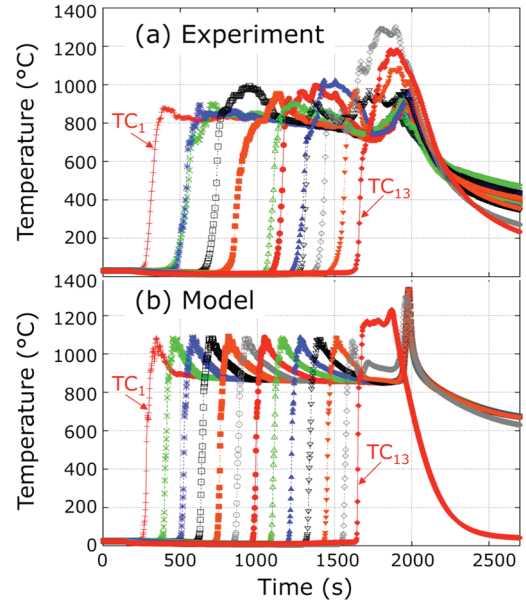

Figure 7. Comparison of temperatures of thermocouples predicted by the GARBED-tr model with those measured experimentally in the batch furnace.

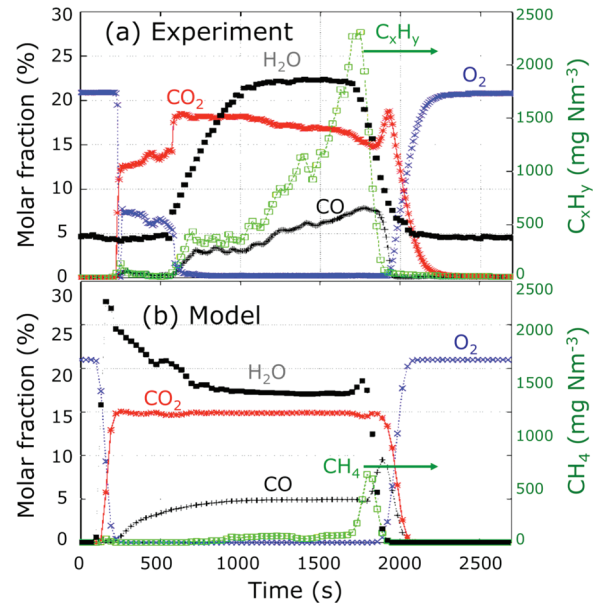

Figure 8. Comparison of evolution of gases above the bed predicted by the GARBED-tr model with that measured experimentally in the batch furnace.

difference concerns water vapor, for which the calculated value shows an early rise, whereas its measured increase is delayed until 600 s. Our explanation is that some condensation likely occurred in the exhaust tube; the gas composition was indeed measured downstream, at the inlet of a postcombustion chamber,

whereas it was calculated at just above the bed. Another difference is in the concentration of hydrocarbons C_xH_y, measured as a whole, whereas the model considers methane, CH_4, to be the only hydrocarbon released in pyrolysis.

Conclusions

A new mathematical model simulating the combustion behavior of an MSW bed on the traveling grate of an incinerator was developed, named GARBED-ss. A two-dimensional, steady-state model, it describes most of the physical, chemical, and thermal phenomena involved: gas and solid flows, heat transfer in and between both phases by convection, conduction, and radiation, drying and pyrolysis of the feed, the oxidation of the pyrolysis gases, the gasification of char by H_2O and CO_2 and its combustion, the reduction in bed volume, and, optionally, stirring of the bed. Several of these features, such as accounting for char gasification and using a two-component, experimentally derived kinetic law for pyrolysis, are specific to our model and represent improvements on those previously proposed. The local momentum, heat, and mass balances are rendered discrete and solved numerically using the finite-volume method, with mesh size decreasing in height according to char consumption. The model, or more precisely its sister version in the transient regime, was validated by successfully comparing calculated solid temperatures and outlet gas composition to the corresponding data from experiments performed in a pilot batch furnace, using wood chips as the fuel.

The set of calculated results (temperature and composition of gas and solid, reaction rates and extents, gas velocity, etc.) give a valuable insight on how waste bed incineration occur. Five zones (fresh feed, dried feed, pyrolysis zone, char, and ash) separated by four fronts and characterized by the principal chemical processes taking place were identified. An important result is the presence of two oxidation fronts, above which stretches a large oxygen-depleted zone in which char is gasified by water vapor and carbon dioxide.

This model can serve as a basis for additional simulations related to the incineration process, such as (i) testing the influence of operating conditions,[14] (ii) using calculated temperatures and compositions for predicting pollutant formation from the bed (e.g., thermodynamic[8] and kinetic[26] calculations on heavy metals), and (iii) coupling the bed model with a model of the remaining sections of the incinerator, with the bed model thus providing the furnace model with accurate boundary conditions.

Acknowledgment

We heartily thank Professor Helmut Seifert, director of ITC-TAB laboratory, Karlsruhe, Germany, for his support and help with the experimental validation of our model. We also acknowledge the financial support of CNRS and ADEME, France, under the aegis of Action de recherche coordonnée "Cycle des métaux lourds lors de l'incinération des ordures ménagères" and Convention ADEME 0372008, and that of Ministère de la recherche for A.A.'s grant.

Supporting Information Available: Additional details, including extra equations, one figure, three tables, and references. This material is available free of charge via the Internet at http://pubs.acs.org.

Literature Cited

(1) Essenhigh, R. H.; Kuo, T. J. Combustion and emission phenomena in incinerators: development of physical and mathematical models of incinerators. Part I: Statement of the problem. *National Incinerator Conference*; Cincinnati, OH, 1970.

(2) Goh, Y. R.; et al. Mathematical modelling of the burning bed of a waste incinerator. *J. Inst. Energy* **1998**, *71*, 110–118.

(3) Shin, D.; Choi, S. The combustion of simulated waste particles in a fixed bed. *Combust. Flame* **2000**, *121*, 167–180.

(4) Yang, Y. B.; Goh, Y. R.; Zakaria, R.; Nasserzadeh, V.; Swithenbank, J. Mathematical modelling of MSW incineration on a travelling bed. *Waste Manage.* **2002**, *22*, 369–380.

(5) Yang, Y. B.; Lim, C. N.; Goodfellow, J.; Nasserzadeh, V.; Swithenbank, J. A diffusion model for particle mixing in a packed bed of burning solids. *Fuel* **2005**, *84*, 213–225.

(6) Ryu, C.; Yang, Y. B.; Nasserzadeh, V.; Swithenbank, J. Thermal reaction modeling of a large municipal solid waste incinerator. *Combust. Sci. Technol.* **2004**, *176*, 1891–1907.

(7) Marias, F. A model of a rotary kiln incinerator including processes occurring within the solid and the gaseous phases. *Comput. Chem. Eng.* **2003**, *27*, 813–825.

(8) Menard, Y.; Asthana, A.; Patisson, F.; Sessiecq, P.; Ablitzer, D. Thermodynamic study of heavy metals behaviour during municipal waste incineration. *Process Saf. Environ. Prot.* **2006**, *84*, 290–296.

(9) Menard, Y. Modélisation de l'incinération sur grille d'ordures ménagères et approche thermodynamique du comportement des métaux lourds. Ph.D. Thesis, INPL, Nancy, 2003; http://tel.archives-ouvertes.fr/tel-00298415/fr/.

(10) Garcia, A. N.; Marcilla, A.; Font, R. Thermogravimetric kinetic study of the pyrolysis of municipal solid waste. *Thermochim. Acta* **1995**, *254*, 277–304.

(11) Dryer, F. L.; Glassman, I. High temperature oxidation of CO and CH_4. *14th Symp. Int. on Combustion*; The Combustion Institute, 1973.

(12) Howard, J. B.; Williams, G. C.; Fine, D. H. Kinetics of carbon monoxide oxidation in postflame gases. *14th Symp. Int. on Combustion*; The Combustion Institute, 1973.

(13) Van Tigellen, P. *Oxydations et Combustions*; Technip: Paris, 1968.

(14) Asthana, A. Modélisation mathématique dela formation des NO_x et de la volatilisation des métaux lourds lors de l'incinération sur grille d'ordures ménagères. Ph.D. Thesis, INPL, Nancy, 2008; http://tel.archives-ouvertes.fr/tel-00285446/en/.

(15) Wakao, N.; Kaguei, S. Heat and mass transfer in packed beds. *Topics in Chemical Engineering*; Gordon and Breach: New York, 1982; Vol. 364.

(16) Donald, B.; Anthony, J. B. H. Coal devolatilization and hydrogasification. *AIChE J.* **1976**, *22*, 625–656.

(17) Arthur, J. R. Reactions between carbon and oxygen. *Trans. Faraday Soc.* **1951**, *47*, 164–178.

(18) Linjewile, T. M.; Gururajan, V. S. CO/CO_2 product ratio from the combustion of single petroleum coke spheres in an incipiently fluidized bed. *Chem. Eng. Sci.* **1995**, *50*, 1881–1888.

(19) Rosendahl, L. A. Extending the modelling framework for gas-particle systems: applications of multiparameter shape descriptions to non-conventional solid fuels in reacting and non-reacting environments. *Institute Energy*; Aalborg University: Aalborg, 1998.

(20) Laurendeau, N. M. Heterogeneous kinetics of coal char gasification and combustion. *Prog. Energy Combust. Sci.* **1978**, *4*, 221–270.

(21) Ryu, C. K.; Shin, D.; Choi, S. Effect of fuel layer mixing in waste bed combustion. *Adv. Environ. Res.* **2001**, *5*, 259–67.

(22) Nakamura, M.; Themelis, J. Modeling of solid waste flow and mixing on the traveling grate of a waste-to energy combustion chamber. *12th North American Waste To Energy Conference (NAWTEC 12)*; Savannah, GA, 2004.

(23) Nakamura, M. Mathematical and physical modeling of mixing and flow phenomena on a reverse acting grate. Ph.D. Thesis, Columbia University, New York, 2008; http://www.seas.columbia.edu/earth/wtert/sofos/nakamura_thesis.pdf.

(24) Patankar, S. V. Numerical heat transfer and fluid flow. *Series in Computational Methods in Mechanics and Thermal Sciences*; Hemisphere Publishing Corp.: New York, 1980.

(25) Falcoz, Q.; Gauthier, D.; Abanades, S.; Flamant, G.; Patisson, F. Kinetic rate laws of Cd, Pb and Zn vaporization during municipal solid waste incineration. *Environ. Sci. Technol.* **2009**, *43*, 2184–2189.

(26) Asthana, A.; Falcoz, Q.; Sessiecq, P.; Patisson, F. Modeling kinetics of Cd, Pb, and Zn vaporization during municipal solid waste bed incineration. *Ind. Eng. Chem. Res.* **2010**, doi: 10.1021/ie100181x.

Received for review January 27, 2010
Revised manuscript received June 23, 2010
Accepted June 25, 2010

IE100175E